



REGISTRATION OF REMOTE SENSING IMAGES BASED ON FEATURE FUSION TECHNIQUES

M. M. Asker

O.. Abu –ElNasr

B. Shabana

S. Elmougy

Faculty of Computers and Information,
Mansoura University, Egypt

Misr Higher Institute for Commerce
and Computer Science,
Mansoura-Egypt.

Faculty of Computers and
Information,
Mansoura University, Egypt

mohammad.asker@gmail.com

abuelnasr@yahoo.com

BahaaShabana@yahoo.com

mougy@mans.edu.eg

Abstract: Geometric correction is used to correct the registration errors in remotely sensed images. These images are often compared to ground control points (GCPs) either by using an accurate map (image to map) or using another geo-referenced image (image to image) and then resampled. Accordingly, the exact locations and the appropriate pixel values can be calculated in more accurate, time-wise and effortless manner. In the traditional methods, the GCPs are manually selected and then the transformation models are applied which yield time consuming and less accurate processes. The objective of this work is to develop an automatic approach for image registration based on another geo-referenced image using five feature extraction models. They are Scale Invariant Feature Transform (SIFT), Speeded Up Robust Features (SURF), Discrete Wavelet Transforms (DWT), (SIFT & DWT), and (SURF & DWT). The GCPs were selected based on the least-squares adjustments as the basis for improving the spatial accuracy of all the linking points in both images. The obtained results showed that models have higher accuracy in image registration with Root Mean Square Error (RMSE) less than 0.5. The developed automated image registration method provides more accurate results and saves time, money and effort.

Keywords: Geometric Correction, GCPs, SIFT, SURF, DWT.

1. Introduction

Remote sensing imagery contains unique geometric distortion either due to acquisition system or the movements of the platform. The sources of these distortions could be grouped into two broad categories: the observer or the acquisition system (platform, imaging sensor and other measuring instruments etc.) and the observed (atmosphere and earth) [1]. Accordingly, there are two types of geometric errors [2]: systematic and non-systematic errors. The first type is generally caused by mirror scans, velocity variance, scan skew, platform velocity, earth rotation, and panoramic distortion and can be corrected through analysis the system characteristics and ephemeris. The non-systematic errors are caused by the position and attitude angles of the satellite platform and can be corrected based on image to map or image to image registration methods [3].

Geometric correction is used to correct the variation between the actual location coordinates and the raw image data on the ground or target image. A number of types of geometric corrections include system,

precision, and terrain corrections could be used. There are four different levels for geometric correction of remotely sensed imagery [4]. These levels are: 1) Registration: alignment of one image to another image of the same area; 2) Rectification: alignment of image to a map so that the image is planimetric, just like the map; which is also known as geo-referencing; 3) Geocoding: a special case of rectification that includes scaling to a uniform standard pixel size; 4) Ortho-rectification: correction of the image, pixel by pixel for topographic distortion. The major image geo-correction techniques [1] are image to map and image to image corrections. The image-to-map uses reference frame such as to po-sheets, maps or any standard spatial reference such as the Universal Transverse Mercator (UTM). The image-to-image method matches one image to another image so that the same geographic area is positioned coincident with respect to the reference image. This type of geometric correction is used when it is not necessary to have each pixel assigned a unique (x, y) coordinate in a map.

Both of SURF, SIFT and DWT techniques are used worldwide in image registration [5] [6]. Image registration main stages are [7]:

1. **Preprocessing:** adapts both the reference image and the input for improving the conduct of the selection of the feature and the correspondence of the feature of registering image. This is due to a number of images could be foggy or may be having an amount of noise that is noteworthy and which will have a dramatic effect on the algorithm's outcome. A number of techniques easing the noise by using Image Restoration and Image Enhancement functions to remove the atmospheric distribution. Also, the canny edge detection filter is used to improve the edges in the image.
2. **Feature Extraction:** chooses the main features like crossroads, edges and lines; which will be used to do feature correspondence. At this stage five methods are used (SIFT, SURF, DWT, SIFT & DWT, and SURF & DWT) for feature extraction.
3. **Feature Matching:** makes a matching between the main chosen features in the image of reference and the target image for finding out what points in the reference image is a match with the points in the target image. The Mutual Information (MI) method for features matching was used in this work.
4. **Transformation Model Estimation:** lines up both target image and reference image through using the function of mapping.
5. **Resampling:** this method is used to estimate Digital Value (DV) to be placed in the new pixel location in the corrected output image. There are three methods of resampling, nearest neighbor, bilinear interpolation, and cubic convolution.

The main objective of this paper is to develop an automatic approach to make image registration based on another geo-referenced image using SURF, SIFT and DWT techniques and their fusion (SURF & DWT) and (SIFT & DWT). The paper is organized in five sections including this section. Section two includes a background about the topic of study and the related work in this field. Section three explains the development of the proposed system. Section four contains the obtained results and their discussions. Section five, which is the last section provides a summary about the main conclusions and recommendations for future work.

2. Background and Related Works

Geometric distortion is a big issue in image based application. It appears as an error in the appearance of an image. The distortion can be classified as either internal distortions or external distortions. The internal distortions result from the geometry of the sensor while external distortions resulting from the attitude of the sensor or the shape of the object. Geometric correction is undertaken to overcome geometric distortions. Automatic registration of remote sensing images is important for implementing a geometric correction that handles the geometric distortions.

Feature based image registration model can be generally decomposed into five basic steps: preprocessing, feature detection, matching, transformation model estimation and image transformation and resampling. Figure 1 shows the basic steps of feature based image registration model.

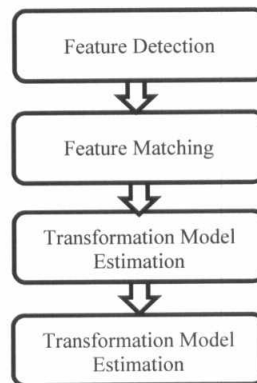


Figure 1: Fundamental steps of feature based image registration [32].

Many of feature based images registration approaches have been proposed and reviewed. Qian (2016) [8], proposed a fast remote sensing image registration technique based on the combination of both the improved AGAST and FREAK techniques. The improved AGAST is used to detect the feature points between the reference image and the target image. He also used the FREAK algorithm to obtain a binary string descriptor and hamming distance between features vector computed by using a cascade match to get well matched feature points. Subha et al. (2015) [9], implemented a feature based image registration approach by using DWT as a feature extraction technique, SIFT as a feature matching technique and normalized cross correlation (NCC) for obtaining maximum positive matches. Jitendra et al. (2015) [10], developed an image registration approach based on extracting wavelet features and optimizing the selection of GCPs using a Particle Swarm Optimization (PSO) technique. Phogat et al. (2015) [11], developed manual and automatic registration approaches and made a comparison between them. They found that the automatic process gave much better and robust result when compared with the manual registration. Elkhachy et al. (2014) [12], investigated the effect of the number of GCPs with various 2D polynomial rectification models on the accuracy of geometric correction. They observed that increasing the number of GCPs improve the registration accuracy. However, this is true as long as the accuracy of the GCPs is homogeneous and is well distributed all over the studied image. Shah et al. (2014) [13], implemented a robust feature selection and matching approach by using several techniques. They are: the Principle Component Analysis (PCA), SURF and SIFT. Xia et al. (2013) [14], proposed an automatic selection approach for control point pairs based on regional matching. This approach detects features by using a scale invariant and rotation invariant SIFT feature descriptor. Fatin (2007) [15], made an enhancement of satellite images by implementing a discrete wavelet technique for Singar mountain region located west of Mosul city in Iraq.

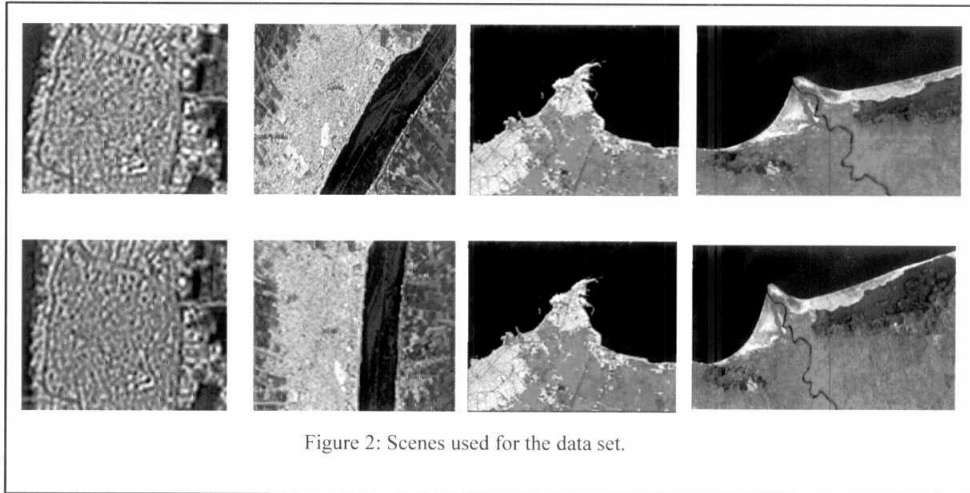


Figure 2: Scenes used for the data set.

3. The Proposed Approach

The main objective of this paper is to develop an automatic approach for image registration based on another geo-referenced image using five feature extraction models: SIFT, SURF, DWT, SIFT & DWT, and SURF & DWT. An image to image registration method is used to make a geometric correction for two Landsat images. Figure 3 demonstrates the proposed model that shows the main procedures used in developing automated image registration model.

The used data set has been decomposed into two sets: reference set and sensed set for Rosetta-Egypt. The reference set has been captured at 2002 and the sensed set captured at 2014 for the same region. Figure 2 shows the reference and the sensed data set respectively. The simulation environment is Matlab R2013a, Intel(R) Core(TM) i3-2310M CPU 2.10GHz, memory size 6.00G on Windows 7 Ultimate.

3.1 Preprocessing

Some images may have an amount of noise that is noteworthy and that has a dramatic effect on the result of the further processing. Preprocessing commonly carries out a series of sequential operations such as image restoration, enhancement, noise removal and edge detection that modify both the target and reference image.

3.1.1 Image Restoration

This operation is used to remove the distortion from the image in order to enhance the visual interpretation of the image. It removes the fog distribution in the remotely sensed images. A model developed by Koschmieder is used to minimize the effect of fog in the image in which $L(x, y)$, the apparent luminance at pixel (x, y) is given by [16]:

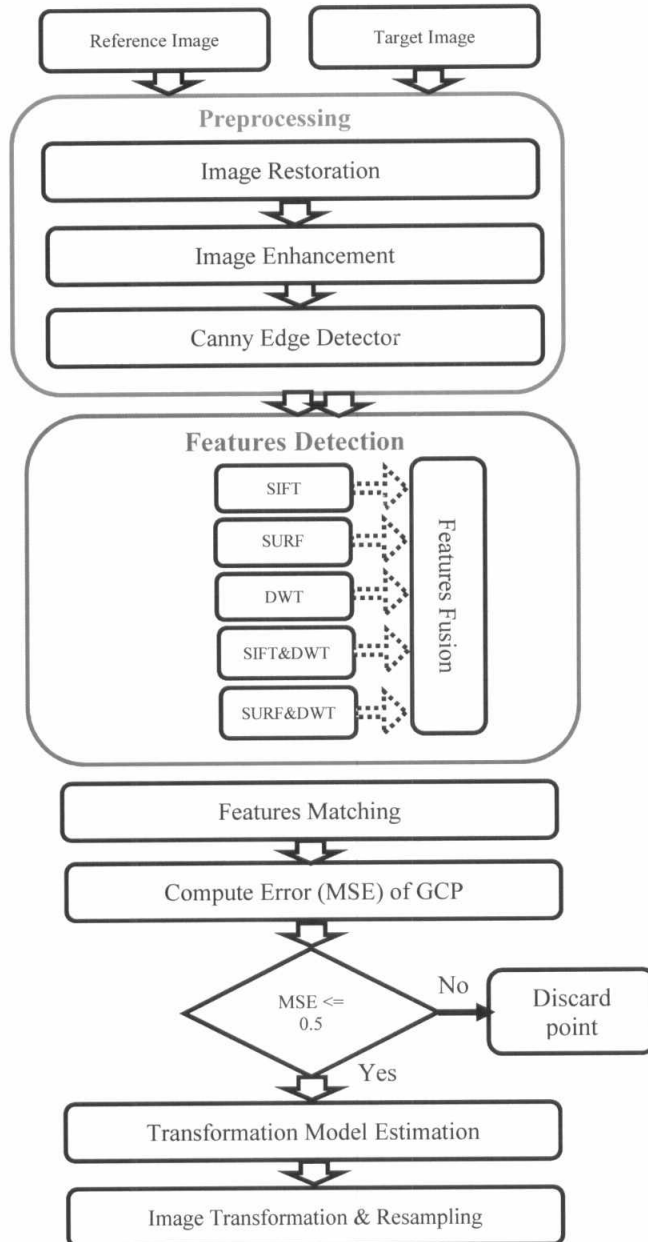


Figure 3 : Flowchart of the procedures used in develop automated image registration model.

$$L(x, y) = L_0(x, y)e^{-kd(x,y)} + L_s(1 - e^{-kd(x,y)}) \quad (1)$$

where $d(x, y)$ is the distance of the corresponding object with intrinsic luminance $L_0(x, y)$, and L_s is the luminance of the sky and k denotes the extinction coefficient of the atmosphere. This model was is this work due to its simplicity and it is fast output. Angle as an alternative to the median filter but other operators dedicated to visibility restoration allowing to infer the atmospheric veil can be also imagined. It also develops a linear function of the input image. Size and it also achieves as good or even better results compared to state of the art algorithms (Kopf and et al [17], Fattal [18], Tan [19]). Also the visibility restoration from a single image without using any extra information as a particular filtering problem. A visual comparison between the input and the output image is resulted from the image restoration process is shown in Figure 4.

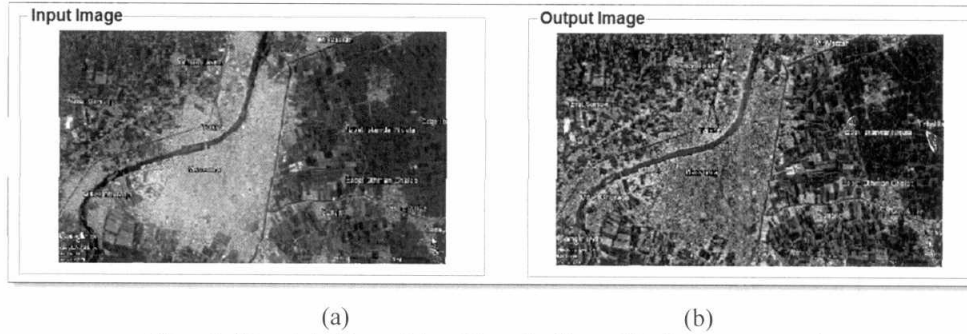


Figure 4 : The original image (a) and the output image (b) after image restoration.

3.1.2 Image Enhancement

The image enhancement operation is used to improve the subjective appearance of an image in order to provide a better transform representation for future processing. A spatial domain histogram equalization technique was used in this work to make a contrast adjustment using the image histogram by increasing the global contrast. As a result, the intensities are well scattered on the histogram and spreading it along the histogram. The histogram equalization technique formula was carried out using the following formula [20]:

$$h(v) = \text{round} \left(\frac{cdf(v) - cdf_{min}}{(m * n) - cdf_{min}} * (L - 1) \right) \quad (2)$$

where $cdf(v)$ is Cumulative Distribution Function of a gray value, cdf_{min} is Minimum CDF value in the image, L is Total gray level in the image and $m * n$ are *width * height* of the image.

Figures 5 and 6 shown both of the appearance and the histogram of the studied satellite images before and after performing the histogram equalization technique.

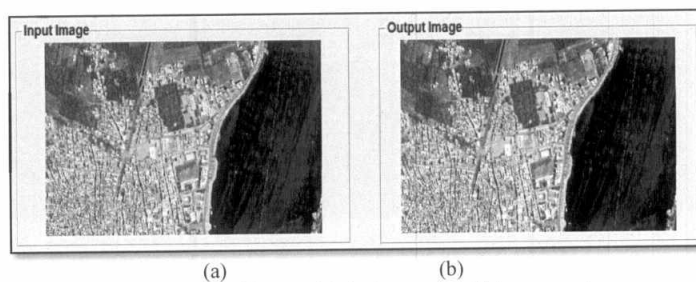


Figure 5: (a) original image (b) the image after Enhancement.

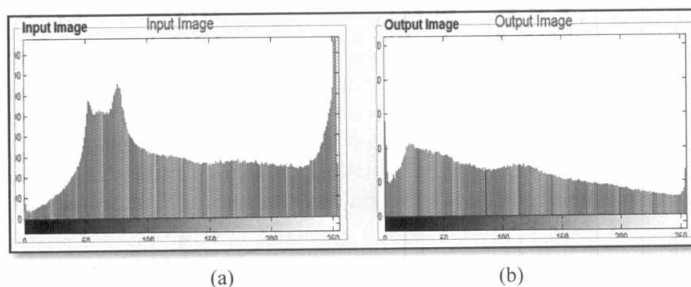
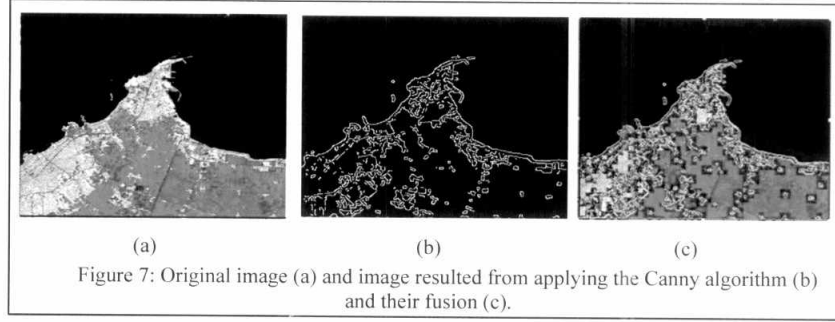


Figure 6: (a) Histogram of original image (b) Histogram equalization of original image.

3.1.3. Canny Edge Detector

Most remote sensing applications use edge detection as a preprocessing stage for feature extraction. Implementing canny edge detector for feature extraction and image enhancement helps in enhancing the corrupted images and extracting the edges. The Canny filter is built based up on sobel filter, which incorporates some pre and post-processing steps to increase the accuracy of edge detection. Figure 5 shows the effect of implementing canny edge detector.

A novel edge-detection algorithm is necessary to provide an errorless solution that is adaptable to the different noise levels in satellite images. The Canny algorithm relies mainly on changing the parameters which are standard deviated for the Gaussian filter and its threshold values. The size of the Gaussian filter is controlled by the greater value and the larger size. The larger size produces more noise, which is necessary for noisy images, as well as detecting larger edges. The Canny algorithm is used in this work because it exhibited better performance when compared with other algorithms such as LoG, Sobel, Prewitt, and Roberts [21] [22]. Figure 7 shows the resulted images from applying the Canny algorithm on the original image and their fusion.



3.2 Feature Extraction

Once the preprocessing steps have been done, the features have to be extracted and then the ground control points (GCPs). The feature space can be formed based either on intensity or feature based methods. The first type manipulates the image by dealing directly with the image pixels as a feature space. The second type extracts a set of feature points from an image and makes use of these only extracted feature points instead of the whole image pixels. In this work, five feature extraction techniques were used. SIFT, SURF, DWT and their fusions (SIFT & DWT) and (SURF & DWT).

3.2.1 SIFT Method

The SIFT method extracts and describes the feature points which are scale invariant, rotation invariant and insensitive to change in illumination [23]. It is implemented as a series of the following four steps:

1. Scale-space extrema detection: It searches over scale space of the image to identify the interest points that are scale invariant and orientation invariant. The scale space $L(x, y, \sigma)$ can be defined by convolving the input image $I(x, y)$ with Gaussian filter $G(x, y, \sigma)$ as given in Equation (3).

$$L(x, y, \sigma) = G(x, y, \sigma) * I(x, y) \quad (3)$$

where, $I(x, y)$ is input image, and $G(x, y, \sigma)$ is variable-scale Gaussian.

Stable Key point locations $D(x, y, \sigma)$ are then obtained as maxima/minima of the difference of Gaussians (DoG) which can be obtained from the difference of two nearby image scales: one with scale k times the other. $D(x, y, \sigma)$ is then given by Equation (4):

$$D(x, y, \sigma) = L(x, y, k\sigma) - L(x, y, \sigma) \quad (4)$$

- 2) Key point localization: In this step, both the scale and the location of each candidate point are determined. These points are proved to have low contrast and poorly localized along an edge.
- 3) Orientation assignments: Depending on local image gradient directions, one or more orientations are assigned to each feature point location. For each image sample at the scale $L(x, y)$, the gradient magnitude $m(x, y)$ and orientation $\theta(x, y)$ can be computed as given in equations (5) and (6), respectively.

$$m(x, y) = \sqrt{(L(x+1, y) - L(x-1, y))^2 + (L(x, y+1) - L(x, y-1))^2} \quad (5)$$

$$\theta(x, y) = \tan^{-1} \left(\frac{L(x, y+1) - L(x, y-1)}{L(x+1, y) - L(x-1, y)} \right) \quad (6)$$

- 4) Key point descriptor: A feature descriptor creates a 16×16 neighborhood that is partitioned into 16 sub regions of 4×4 pixels each. For each pixel within a sub region, SIFT adds the pixel's gradient vector to a histogram of gradient directions by quantizing each orientation to one of 8 directions and weighting the contribution of each vector by its magnitude. Figures 9 and 10 shown the outputs of feature extraction and image registration resulted from applying the SIFT transform technique.

3.2.2 Speeded Up Robust Feature Detector (SURF)

SURF detects and describes the image that is vigorous. The detector of SURF is chiefly grounded on the estimated Hessian Matrix [24]. Conversely; the descriptor distributes the responses of Haar-wavelet within the points of neighborhood interest. The detector and the descriptor are both utilized for reducing the time for computing as the descriptor is dimensionally low. As a result, the SURF shows a better performance than the used schemes that were used before regarding repeatability, uniqueness, heftiness and rapidity [24].

SURF generates a "stack" without 2:1 down sampling for levels that are higher in the pyramid which results in images that have a resolution that is similar. SURF filters the stack using a box filter approximation of second-order Gaussian partial derivatives [25] since integral images allow the computation of rectangular box filters in near constant time. The nearest neighbor is distinct to be the key-point with least Euclidean distance for the vector of the invariant descriptor [26]. The Gaussian second order partial derivative box filters of D_{YY} and D_{XY} are shown in Figure 8.

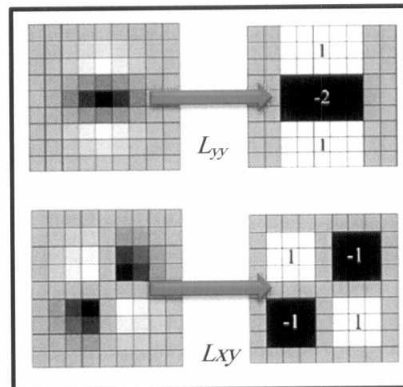


Figure 8: Gaussian second order partial derivatives [26] [25].

3.2.2.1 Fast Hessian Detector

SURF detector is grounded on the metrics of Hessian that reasons a decent act and correctness. Supposing that for an image I , $X = (x, y)$ is the point that is given, then the Hessian metrics $H(x, \sigma)$ for X which has the scale σ , is distinct as proven in Equation (7) [24]

$$H(x, \sigma) = \begin{bmatrix} L_{xx}(x, \sigma) & L_{xy}(x, \sigma) \\ L_{xy}(x, \sigma) & L_{yy}(x, \sigma) \end{bmatrix} \quad (7)$$

where, $L_{xx}(x, \sigma)$ is the convolution of the Gaussian second order derivative with the image I in point x , and similarly for $L_{xy}(x, \sigma)$ and $L_{yy}(x, \sigma)$.

In estimated Hessian detector, an estimated Hessian matrix by means of box filter is utilized in place of just Hessian matrix like illustrated in Figure 8. At this point, 9×9 box filter is utilized having $\sigma = 1.2$ [25] [26]. Typically, there is a normalization of the filter response regarding the size of the mask.

3.2.2.2 SURF Descriptor

In the first step of SURF descriptor, to extract the feature points, and fix a reproducible orientation based on information from a circular region around the interest point. After, it builds a square region aligned to the selected orientation. To become the invariant to rotation, it calculates the Haar - Wavelet which responses in x and y direction as shown in Figure 9.

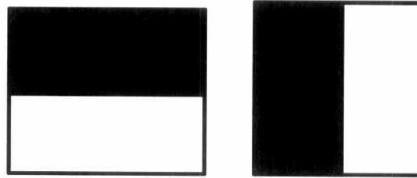


Figure 9: Harr - wavelet types used for SURF [26].

There could be a processing of it in a circular neighborhood of radius $6s$ about the points of attention, where s symbolizes the detection of the attention points scale. By means of a calculation of all responses of the sum within a descending alignment window that covers a 60 degree [13], the leading alignment is expected. The next phase is to sum responses that are both horizontal and vertical inside the window. Here, the result is known as a novel vector. The longest such vector gives its alignment to the point of interest.

3.2.3 Discrete Wavelet Transforms (DWT)

The wavelet transform is a temporal multi-resolution feature descriptor. It captures both frequency and location information. The wavelet transform generates a multi-resolution representation of image data. Wavelet-based multi-resolution preserves most of the important features of the original data. It also eliminates weak features in higher resolution, whereas it highlights strong image features [27]. Wavelet is a mathematical process that is used to obtain approximate and detailed coefficients from decompose signals. These coefficients allow the signal to be described in several levels from the coarse level to the finest level. Generally, the functionality of wavelets in 2D depends on passing the original image columns through high-pass and low-pass filters. After, the rows of the filtered image are passed through high-pass and low-pass filters [28]. The approximate coefficients will be used to transform the image in case if the image is transformed by another level. Each pass through the filter decreases both the column and row by two [28]. This process keeps repeating until the process has reached n levels (which is

specified by the user and in our algorithm we assume that $n = 1$) [29]. After the Wavelet analysis decomposition has been completed, the image is divided into four sub-images: approximate, horizontal, vertical, and diagonal.

As soon as we get the foundation function we can define the DWT for the image using Equation (8) - Equation (11) where $M, N, H, V, D, W_\phi(j_0, m, n), w_\psi^H(j, m, n), w_\psi^V(j, m, n), w_\psi^D(j, m, n)$ refers to the number of columns, number of rows in the image, horizontal, vertical, diagonal, approximate coefficients at scale j_0 which is usually equal to θ , horizontal, vertical, and diagonal detail coefficients at scale j in which j, j_0 correspondingly.

$$W_\phi(j_0, m, n) = \frac{1}{\sqrt{MN}} \sum_{x=0}^{M-1} \sum_{y=0}^{N-1} f(x, y) \phi_{j_0, m, n}(x, y) \quad (8)$$

$$w_\psi^H(j, m, n) = \frac{1}{\sqrt{MN}} \sum_{x=0}^{M-1} \sum_{y=0}^{N-1} f(x, y) \psi_{j, m, n}^H(x, y) \quad (9)$$

$$w_\psi^V(j, m, n) = \frac{1}{\sqrt{MN}} \sum_{x=0}^{M-1} \sum_{y=0}^{N-1} f(x, y) \psi_{j, m, n}^V(x, y) \quad (10)$$

$$w_\psi^D(j, m, n) = \frac{1}{\sqrt{MN}} \sum_{x=0}^{M-1} \sum_{y=0}^{N-1} f(x, y) \psi_{j, m, n}^D(x, y) \quad (11)$$

where, m, n, H, V and D , represent the number of columns in the image, number of rows in the image, horizontal, vertical, diagonal, approximate coefficients at scale j_0 which is usually equal to θ , horizontal, vertical, and diagonal detail coefficients at scale j where $j \geq j_0$ respectively [30]

3.2.4 Feature Fusion

Features fusion technique forms the feature space as a combination of features from multiple sources. Feature fusion is used to achieve more specific inferences than these achieved by using only a single source. In this work, a feature space is built based on a combination of (SIFT and DWT) and (SURF and DWT) models. Figure 10 shows the flowchart of applying these two fusion models.

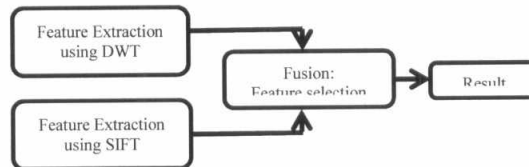


Figure 10: Flowchart of proposed fusion method.

3.3 Feature Matching

Once the feature spaces have been built, the correspondence between those extracted to label the target image and those extracted to label the reference image is established. MI based approach has developed

recently and it represents a leading technique in images registration [5]. MI is a measure of statistical dependency between two datasets as shown in Figure 11. It is particularly suitable for registration of images obtained from different modalities. MI between two random variables X and Y is calculated using the following equation:

$$MI(X, Y) = H(Y) - H(Y | X) = H(X) + H(Y) - H(X, Y) \quad (12)$$

where $H(x) = -E_x(\log(P(X)))$ represents entropy of random variable and $P(X)$ is the probability distribution of X .

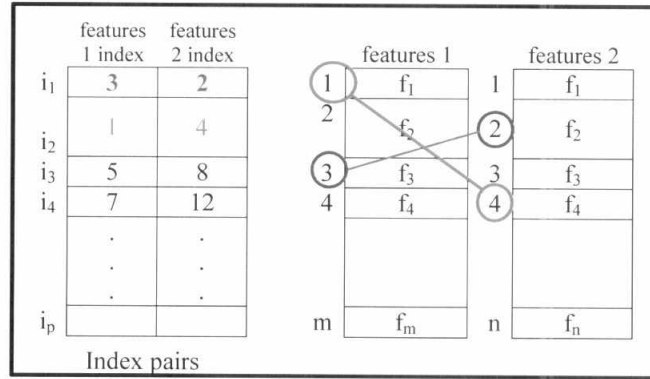


Figure 11: Feature matching between any two datasets [13].

3.4 Accuracy Assessment

Registration evaluation intends to give a decision about the accuracy of the implemented model. The assessment of registration accuracy determines whether the image registration is correctly achieved or there are registration errors. For registration accuracy, statistical parameters such as x-residual, y-residual, Root Mean Square Error (RMSE) and Mean Square Error (MSE) are used as follow [31]:

$$RMSE(in x) = \sqrt{\sum_{i=1}^n (\Delta X_i)^2} \quad (13)$$

$$RMSE(in y) = \sqrt{\sum_{i=1}^n (\Delta Y_i)^2} \quad (14)$$

$$RMSE_T = \sqrt{\frac{1}{n} \sum_{i=1}^n (\Delta X_i^2 + \Delta Y_i^2)} \quad (15)$$

Where: $\Delta X_i, \Delta Y_i$ = residuals of point (i) in X and Y directions, T = total RMS error, n = number of GCPs,
 i = GCP number.

In this work, only $RMSE$ was used for assessment of registration accuracy. Once, $RMSE$ is calculated, the point pairs that cause an increase in the $RMSE$ value are removed. In case if the total $RMSE$ is still too large, another round of consistency checks is executed. The iteration continues to run until the $RMSE$ value is less than the proposed threshold which is 0.5 of pixels.

3.5 Estimation of Transform Model

The estimation of the transformation parameter is a crucial step in the registration process of remotely sensed images. The required parameters needed for the mapping function are assigned in this step. These parameters are obtained from the calculated feature pairs for the correspondences, which were built through feature matching.

3.6 Image Transformation and Resampling

Image transformation is the transformation of the slave image coordinate system into the master image coordinate system. The mapping of any point $[x_1, y_1]$ in the slave image to $[x_2, y_2]$ in the master image is modeled as:

$$x_2 = f(x_1, y_1 | \alpha) \quad (16)$$

$$y_2 = (x_1, y_1 | \beta) \quad (17)$$

where, α and β are the parameters of the mapping function and x_1, y_1 , respectively, which are determined by the control points [32].

Resampling refers to the method that is used to estimate DV to be placed in the new pixel location in the corrected output image. Three resampling methods are used for that purpose: nearest neighbor, bilinear interpolation, and cubic convolution [7].

4. Results and Discussions

Five feature image based registration models were carried out in this work. These models are SIFT, SURF, DWT, (SIFT & DWT), and (SURF & DWT). Figures 12 and 13 shown the results of feature extraction and image registration obtained from implementing SIFT model. Although SIFT technique is having lots of advantages but its performance is degraded for textured scene or when the edges are not reliable [33]. In other words, SIFT model is less sensitive in recognizing the edges of the image. Therefore, Canny edge detection filter is used to facilitate this process. Getting rid of the noise is a very essential part for our approach in order not to get inefficient or false matching.

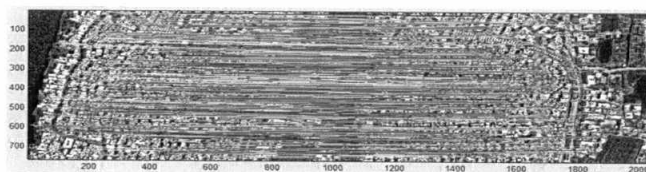


Figure 12: Feature extraction resulted from using the (SIFT) method.



Figure 13: Image registration resulted from the SIFT transform

Figures 14 and 15 shown the results of feature extraction and image registration obtained from carrying out the SURF model. This model is a modified version of the SIFT model. It has many advantages over the SIFT model such as the identifying the number of features, the processing time, and the overall accuracy. The number of features to be extracted can pre-assigned in SURF model in which it has shorter time and experience higher accuracy when compared with the SIFT model.

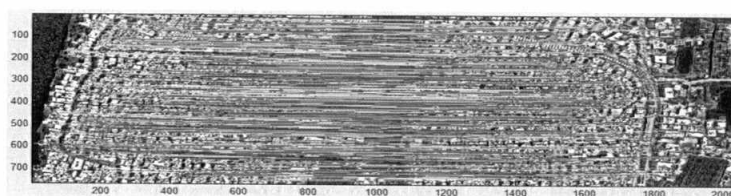


Figure 14: Feature extraction resulted from using the SURF method.

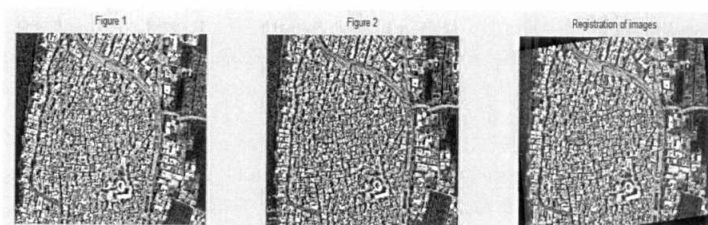


Figure 15: Image registration resulted from the SURF transform technique.

Figures 16 and 17 shown the results of feature extraction and image registration obtained from carrying out the SURF model. This model is a modified version of DWT model. DWT is a robust model in which it shows better results when compared with SIFT and SURF models.

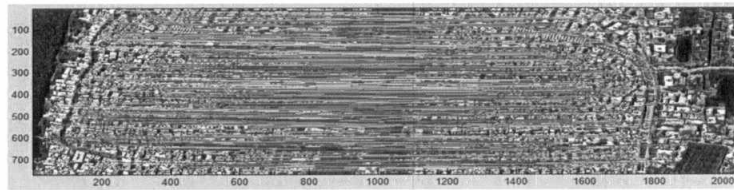


Figure 16: Feature extraction resulted from using the DWT method.

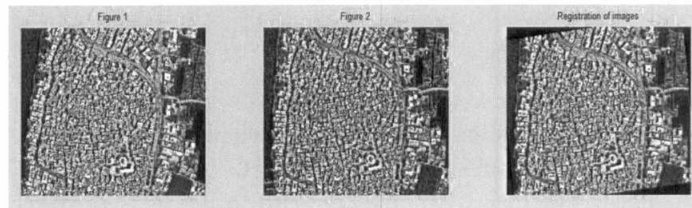


Figure 17: Image registration resulted from the DWT transform technique.

Figures from 18 to 21 shown the results of feature extraction and image registration acquired from performing the two used model fusions (SIFT & DWT and SURF & DWT). These two model fusions showed better results when compared with each individual model. However, they took a relatively long time.

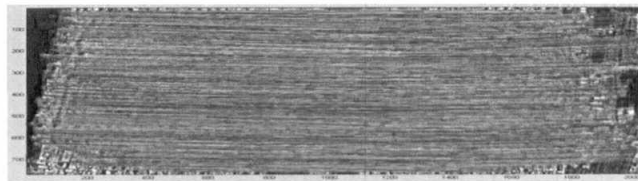


Figure 18: Extraction result of the third proposed method (SIFT & DWT).

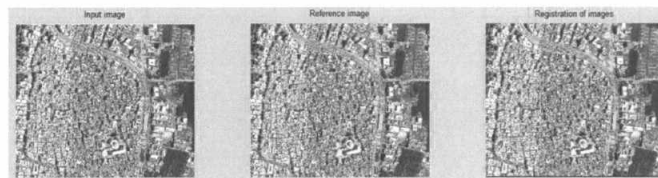


Figure 19: Registration of images : result of features fusion technique (SIFT & DWT).

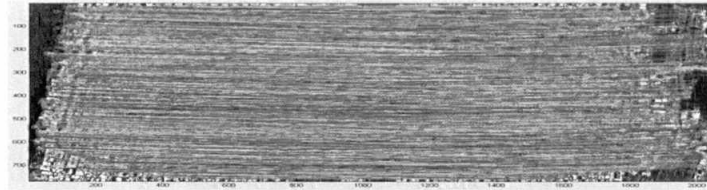


Figure 20: Extraction result of the third proposed method (SURF & DWT).



Figure 21: Registration of images : result of features fusion technique (SURF & DWT).

The quantitative results obtained from implementing the five studied models are represented in Table1. These models were compared based on RMSE, computational complexity, registration accuracy and number of matching feature points. It was found that the (SURF & DWT) had the lowest RMSE value (0.313) followed by (SIFT & DWT), DWT, SURF and SIFT respectively as shown in Figure 22. However, the number of matching feature points increased in this direction the (SIFT & DWT) < DWT<SIFT< SURF<(SURF & DWT) as demonstrated in Figure 24. It was also found that the two model fusions (SIFT & DWT and SURF & DWT) took larger time when compared with the other three models as represented in Figure 25. Both of SURF & DWT and SIFT & DWT didn't have a significant difference in their feature matching time. SIFT model showed the highest number of detected feature points followed by SURF & DWT, SIFT & DWT, DWT and SURF models, respectively. However, number of detected feature points can be pre-assigned in the case of using SURF model and it was given 1000 points in this work. Figure 23 shows the variations among the studied models in the number of detected feature points.

Table 1. Results of the five studied models (SIFT, SURF, DWT, (SIFT & DWT) and (SURF & DWT)) in image registration.

Model based	Detected feature Points		Matching feature point	Feature matching Time (Sec)	RMSE
	Target	Reference			
SIFT	23961	23844	126	23.9	0.417
SURF	1000	1000	180	21.8	0.402
DWT	13204	14130	95	22.6	0.389
(SIFT&DWT)	15890	15527	85	27.6	0.319
(SURF&DWT)	1652	1603	203	26.8	0.313

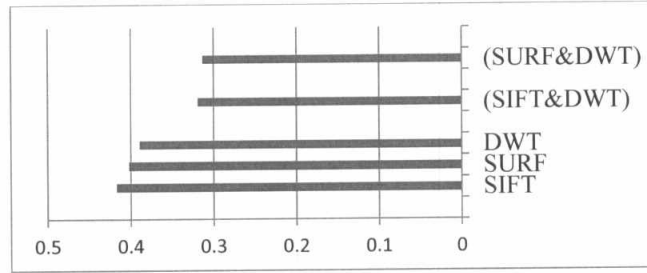


Figure 22: Calculated RMSE for the five studied models.

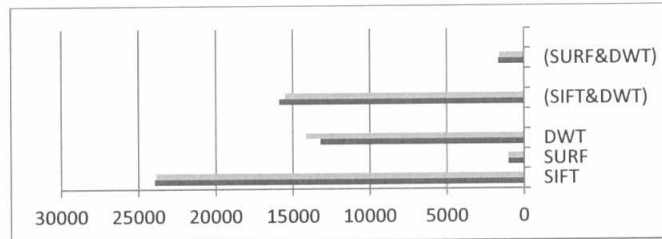


Figure 23: Number of detected feature Points in the target and reference images.

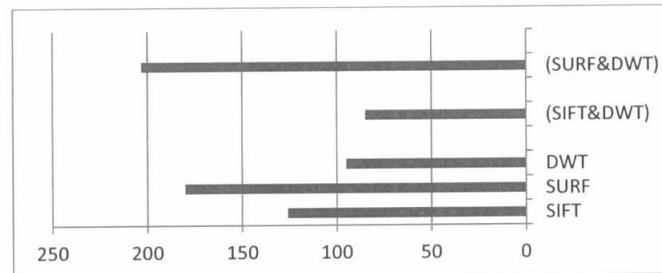


Figure 24: Number of matching feature point in the target and reference images.

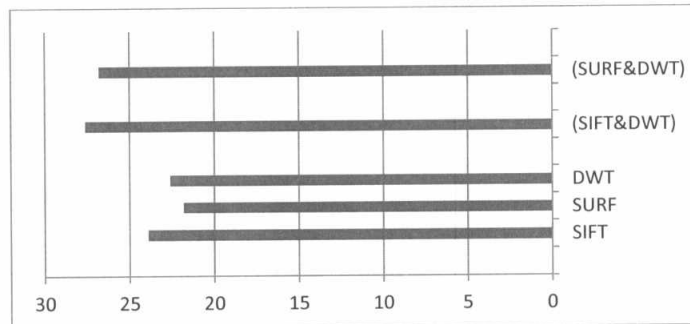


Figure 25: Feature matching time for the five studied models.

5. Conclusion

The proposed automated image registration system in this work based on five studied models (SITF, SURF, DWT, SIFT & DWT and SURF & DWT) showed highly accurate results according to RMSE. This could be attributed to the pre-assigned threshold value where all pairs of GCPs that have a RMSE value 0.5 or greater were discarded in this system. However, there were slight variations among these models regarding to the RMSE values. SURF & DWT had the lowest RMSE value followed by SIFT & DWT, DWT and the SURF and the SIFT, respectively. Also, there were variations among these models in the number of detected feature points, matching feature points, and feature matching time. In general, the two model fusions (SURF & DWT) and (SIFT & DWT) showed better results when compared with each individual model. In the future, an expert image registration system needs to be developed in the field of remote sensing to take the training data from a smaller area and extrapolate them to a larger area or the whole image. This is to save time, effort, money and enhance the overall registration accuracy.

References

1. C. P. Dave, J. Rahul and S. S. Srivastava, "A Survey on Geometric Correction of Satellite Imagery" *International Journal of Computer Applications*, vol. 116, no. 12, pp. 24-27, April 2015.
2. N. Panigrahi, K. M. B and G. Athithan, "Pre-processing Algorithm for Rectification of Geometric Distortions in Satellite Images" *Defence Science Journal, DRDO*, vol. 61, no. 2, pp. 174-179, 2011.
3. Chaudhuri and debasish, Hybrid Image Classification Technique for Land-cover Mapping in the Arctic Tundra, North Slope, Alaska, The University of North Carolina at Greensboro. College of Arts & Sciences: Geography: ProQuest, 2008.
4. P. C. Dave, R. Joshi and S. S. Srivastava, "A Survey on Geometric Correction of Satellite Imagery" *International Journal of Computer Applications*, vol. 116, no. 12, pp. 24 - 27, 2015.
5. V. H. Gandhi and R. S. Panchal, "Feature Based Image Registration Techniques: An Introductory Survey" *International Journal of Engineering Development and Research, IJEDR1401064*, vol. 2, no. 1, pp. 368-375, 2014.
6. C. Paulson, S. Ezekiel and D. Wu, "Wavelet-Based Image Registration" in *Evolutionary and Bio-Inspired Computation: Theory and Applications IV*, Orlando, Florida, 2010.
7. N. Levin, Fundamentals of Remote Sensing, Italy: IMO - International Maritime Academy, 1999.
8. Z. W. a. X. H. Shejun Qian, "Fast Registration of Remote Sensing Image Based on Corner Feature" *Journal of Image and Signal Processing*, vol. 5, no. 1, pp. 43-51, 2016.
9. P.Subha, "Automatic Feature Based Image Registration using DWT and SIFT" *International Journal of Engineering Science and Computing (IJESC)*, vol. 10.4010/2014.165, no. 2321 - 3361, pp. 454 - 457, April 2014.
10. J. Pramanik, S. Dalai and D. Rana, "Image Registration using Discrete Wavelet Transform and Particle Swarm Optimization," (*IJCSIT*) *International Journal of Computer Science and Information Technologies*, vol. 6, no. 2, pp. 1521-1525, 2015.
11. R. S. Phogat, H. Dhamecha and M. Pandey, "Automatic Registration of Satellite Images" *International Journal of Computer Applications*, vol. 120, no. 12, pp. 18-21, June 2015.

12. E.-D. Ismail Elkharchy and Tarek A.E., "Geometric Correction for Very High Resolution Satellite Images" *Civil Engineering Research Magazine (CERM), Al-Azhar University*, vol. 10, pp. 1-15, 2014.
13. U. Shah, D. Mistry and Y. Patel, "Survey of Feature Points Detection and Matching using SURF, SIFT and PCA-SIFT" *Journal of Emerging Technologies and Innovative Research (JETIR)*, vol. 1, no. 1, pp. 35-41, June-2014.
14. Y. Xia and X. Tang, "Extracting Method of Control Point Pairs for Remote Sensing Image Based on Regional Matching" *International Journal of Signal Processing, Image Processing and Pattern Recognition*, vol. 6, no. 2, pp. 145-154, April, 2013.
15. F. Aziz, "Rectification of Satellite Images by Using Wavelet Transform" *Iraq Academic Scientific*, vol. 1, no. 12, pp. 215-228, 2007.
16. H. N, J. P. Tarel, J. Lavenant and D. Aubert, "Automatic fog detection and estimation of visibility distance through use of an onboard camera" *Machine Vision and Applications*, vol. 17, no. 1, pp. 8-20, April 2006.
17. J. Kopf, B. Neubert, B. Chen, M. Cohen, D. Cohen-Or, O. Deussen, M. Uyttendaele and D. Lischinski, "Model-based photograph enhancement and viewing" *ACM Transactions on Graphics (SIGGRAPH Asia'08)*, vol. 27, no. 5, p. 116:1–116:10, 2008.
18. R. Fattal, "Single image dehazing" *ACM Transactions on Graphics (TOG)*, vol. 27, no. 3, pp. 1-9, 2008.
19. R. Tan, "Visibility in bad weather from a single image" *IEEE Conference on Computer Vision and Pattern Recognition*, pp. 1-8, 2008.
20. Brindha, Bharathi, Anusuya and P. Karunya "IMAGE ENHANCEMENT TECHNIQUES: A REVIEW," *International Journal of Research in Engineering and Technology(IJRET)*, vol. 04, no. 05, pp. 455-459, May-2015.
21. R. Maini and H. Aggarwal, "Study and Comparison of Various Image Edge Detection Techniques" *International Journal of Image Processing (IJIP)*, vol. 3, no. 1, pp. 1-9, 2009.
22. G. Shrivakshan, "A Comparison of various Edge Detection Techniques used in Image Processing" *IJCSI International Journal of Computer Science Issues*, vol. 9, no. 5, pp. 269-276, September 2012 .
23. D. G. Lowe, "Distinctive image features from scale-invariant key points" *International Journal of Computer Vision*, vol. 60, no. 2, pp. 91-110, 2004.
24. H. Bay, T. Tuytelaars and L. V. Gool, SURF: Speeded Up Robust Features, 9th European Conference on Computer Vision, Graz, Austria: springer, 2006, pp. 404-417.
25. P. M. Panchal, S. R. Panchal and S. K. Shah, "A Comparison of SIFT and SURF" *International Journal of Innovative Research in Computer and Communication Engineering*, vol. 1, no. 2, pp. 323-327, 2013.
26. A.-L. Kim, J.-H. Song, S.-L. Kang and W.-K. Lee, "Matching and Geometric Correction of Multi-Resolution Satellite SAR Images Using SURF Technique" *Korean Journal of Remote Sensing*, vol. 30, no. 4, pp. 431-444, 2014.
27. S. Mallat, "A Theory for Multi-resolution Signal Approach" *Journal of Photogrammetry and Remote Sensing*, vol. 59, no. 5, pp. 645-653, 1993.
28. C. Paulson, "Wavelet-Based Image Registration" *springer, Communications in Computer and Information Science, CCIS*, vol. 147, pp. 55-60, 2011.

29. J.-S. C. a. J.-M. G. Chih-Hsien Hsia, Multiple Moving Objects Detection and Tracking Using Discrete Wavelet Transform, Discrete Wavelet Transforms - Biomedical Applications, Prof. Hannu Olkkonen (Ed.), ISBN: 978-953-307-654-6, InTech, DOI: 10.5772/15772, 2001.
30. R. Woods and R. Gonzalez, Digital Image Processing, vol. third, Prentice Hall, 2008.
31. B. Zitova and J. Flusser, "Image Registration Methods: a survey" *elsevier, Image and Vision Computing*, vol. 21, no. 2003, p. 977–1000, 2003.
32. Q. Du, N. Raksuntorn, A. Orduyilmaz and L. M. Bruce, "Automatic registration and mosaicking for airborne multispectral image sequences" *Photogrammetric Eng. & Remote Sensing*, vol. 74, no. 2, pp. 169-181, 2008.
33. C. Schmid, "Evaluation of Interest Point Detectors" *International Journal of Computer Vision*, vol. 37, no. 2, p. 151–172, 2000.